

# INTERNAL CASK-CONTENT-COLLISIONS DURING DROP TEST OF TRANSPORT CASKS FOR RADIOACTIVE MATERIALS

Thomas Quercetti, Viktor Ballheimer, Bernhard Droste, Karsten Müller

Federal Institute for Materials Research and Testing (BAM), Berlin, Germany

## ABSTRACT

In transport casks for radioactive materials significantly large axial and radial gaps between cask and internal content are often present because of certain specific geometrical dimensions of the content (e.g. spent fuel elements) or thermal reasons. The possibility of inner relative movement between content and cask will increase if the content is not fixed. During drop testing these movements can lead to internal cask-content-collisions causing significantly high loads on the cask components and the content itself. Especially in vertical drop test orientations onto a lid side of the cask an internal collision induced by a delayed impact of the content onto the inner side of the lid can cause high stress peaks in the lid and the lid bolts with the risk of components failure as well as impairment of the leak tightness of the closure system.

This paper reflects causes and effects of the phenomenon of internal impact on the basis of experimental results obtained from instrumented drop tests with transport casks and on the basis of analytical approaches. Furthermore the paper concludes the importance of consideration of possible cask-content-collisions in the safety analysis of transport casks for radioactive materials under accident conditions of transport.

## INTRODUCTION

Technological gaps from basket or radioactive content to cask body or lid can be a reason for significant dynamic loadings of cask components and its internals due to additional impact interactions in the cask cavity. Different aspects of this issue were discussed in [1-3] on the basis of BAM Federal Institute for Materials Research and Testing experience as competent authority within safety assessment of transport casks for radioactive materials. Experimental results from drop tests conducted by BAM as well as associated calculation results were presented in these publications. The deformation energy stored in the structure before release of the cask in drop test is identified as the main cause of different motion of the cask and its content during the free fall phase and their subsequent impact interactions in the deceleration phase of the drop event [1, 2].

Two simplified approaches considering the interaction between the cask and its internals have been presented recently in [4, 5]. The main objective of the parameter study conducted in [4] was the examination of relationship between cask accelerations and those experienced by the cask content. Among other factors, the gaps in the cask cavity were varied in this study. In [5] a simple dynamic model was used to estimate the effect of gaps on the loading of a cask lid. Admittedly, despite some interesting observations and conclusions discussed in [4, 5] there is no experimental verification for both approaches and so only common recommendations or conservative estimations can be derived from them.

It should be emphasized that any adjustment of the cask and its content relative to one another in the "before drop" configuration (e.g. setting the maximum possible gaps), as required in [5], is not practicable, especially in the drop tests with full scale models of heavy casks. Furthermore, it is obvious that the exact reproducibility of such multiple mass interactions in drop tests is hardly possible as well, because of the rather random nature of the parameters governing these interactions. The differences in the test results of full and reduced scale models [3] can support this conclusion. On the other hand, just due to a multitude of the governing parameters an only numerical analysis of this subject seems to be uncertain. In this context the combination of drop tests with post-test numerical analysis is generally preferred in order to estimate the possible multiple mass effects in a more realistic way.

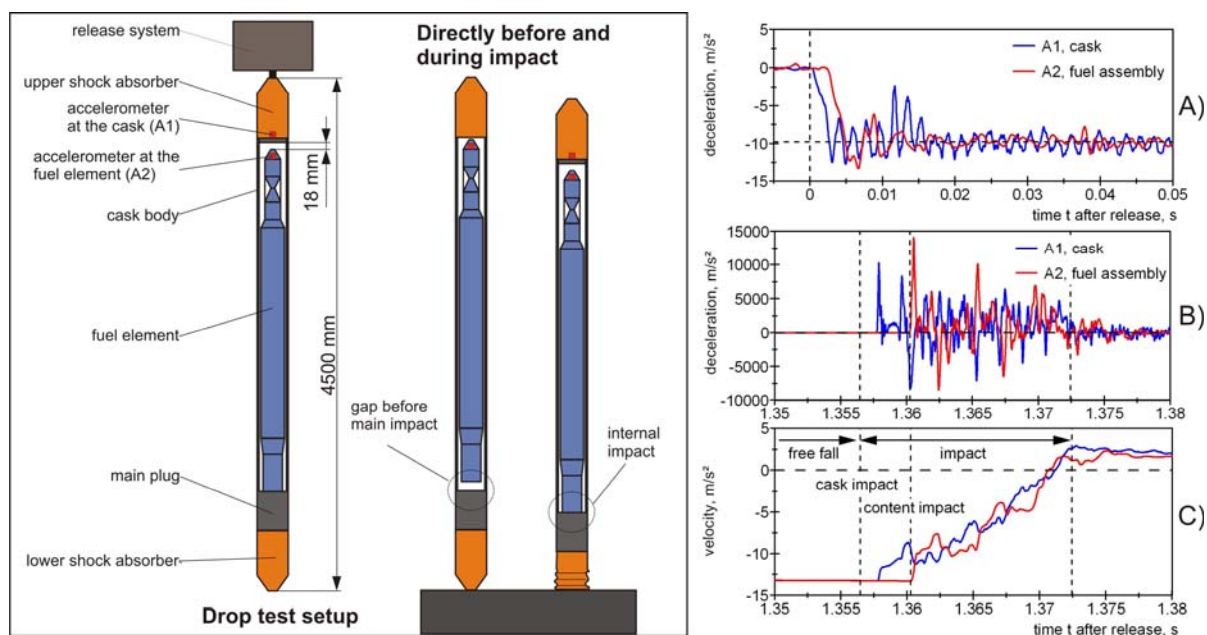
An example of such combined procedure is given in this paper based on a 9 m-vertical drop test with a heavy transport cask for spent fuel elements conducted by BAM. The phenomenology of

the multiple mass effects is illustrated with experimental data from other drop tests showing the cause of different motion between cask and its content.

## PHENOMENOLOGY

The phenomenology of internal cask content collisions will be discussed using the example of an experimental vertical 9 m- drop test with a light transport cask. The cask, labelled ‘ESBB’, was developed by NCS (Nuclear Cargo + Service GmbH) for the transport of single spent fuel assemblies of the SNR 300 fast breeder reactor and is licensed as Type B(U) package [6]. In the context of the corresponding German licensing procedure some years ago the full-scale cask was subjected to several IAEA-drop test sequences with different cask drop orientations. The two vertical drop tests – first drop test onto the cask’s bottom side and second test onto the region of the cask’s main plug – clearly showed the interactions between cask and content. This was evidently illustrated by the first test induced large deformations of the bottom part of the fuel assembly dummy, that could only be explained by a delayed strike of the dummy onto the cask bottom [1, 2]. The delayed interaction and internal impact, respectively, between fuel assembly dummy and cask bottom were also reflected by the signals of the accelerometers which were attached at the content and cask as well. In the second test the accelerometer signals were not only recorded during the main impact onto the target but also during release and free fall of the cask. With these experimental data mechanisms causing internal movement between cask and content could be plausibly explained. In the following this experimental data will be presented in order to complete the analytical approach in [1, 2].

**Figure 1. Drop test setup showing the cask attached to the release system as well as the phase of first contact and internal impact. Deceleration- and velocity-time history of cask and content.**



### *Cask design/ drop test setup/ cask instrumentation*

The ESBB cask consists of a stainless steel tube closed by a welded bottom plate and a welded main plug at the top side. Bottom and main plug are protected by shock absorbers. The specimen was loaded with a fuel assembly dummy. The main dimensions of the cask are 159 mm as outer diameter with a tube wall thickness of 10 mm and 4538 mm as total length. The weights for the dummy fuel element and for the loaded cask were 140 kg and 340 kg, respectively. The SNR 300 fuel assembly has a length of 3680 mm (more details see [6]). The maximum gap in the cavity of the cask between fuel assembly dummy and plug or bottom amounts to approximately 18 mm due to their specific geometries.

Figure 1 shows the drop test setup for the 9 m drop test with the cask’s main plug downwards. The cask is attached with its bottom side upwards to the release system. On the bottom side of the cask body (measurement point A1) and in the foot of the fuel assembly (measurement point A2) one-axis

accelerometers with a built-in mechanical filter system and a 5000 g full-scale output range were mounted. In order to realize high resolution measurement of the lower accelerations during release and free fall, respectively, as well as of the higher accelerations during impact, the accelerometer-signals were branched into two amplifiers (bandwidth 200 kHz) each with a different input range. The low accelerations could be measured with a range of  $\pm 20 \text{ m/s}^2$  - and the higher accelerations with the full range of the accelerometers, i.e.  $50\,000 \text{ m/s}^2$ . The time parameters of the data acquisition device covered the recording during release of the package, the 9 m free fall and the impact. The analogue signals were sampled with 500 kHz and 12 bit.

#### *Causes and effects of the internal impact*

Diagram A of Figure 1 shows the deceleration-time history of the cask body and the fuel assembly dummy during a time window of 5 Milliseconds before and 50 Milliseconds after release, where time  $t$  for  $t = 0$  indicates the starting point of release. The deceleration signals  $A1(t)$  and  $A2(t)$  clearly show a delayed motion of the fuel assembly (A2) relative to the cask (A1) - effects of time shift because of differences in shock wave propagation can be neglected due to the fact that both accelerometers were located very close together. It can be observed that after release ( $t = 0$ ) the fuel assembly keeps in neutral state (deceleration = zero) for a time of two milliseconds while the cask body immediately accelerates to a constant acceleration of  $9.81 \text{ m/s}^2$  - the acceleration due to gravity. After these two milliseconds the cask body as well as the fuel assembly are in a state of free fall - the corresponding signals  $A1(t)$  and  $A2(t)$  oscillate in their natural longitudinal vibration mode about the constant due to gravity - but with different "initial" velocities. This small velocity difference  $\Delta v$  based on the delay of the fuel assembly leads during the free fall of 9 meters with its falling time of 1.3 seconds to a significant gap  $\Delta s$  between cask and content, when the cask body first impacts the target. The internal impact of the fuel assembly occurs 6 milliseconds delayed to the main impact. This effect can be clearly seen in the corresponding acceleration-signals shown in Diagram B of Figure 1. While the cask is already decelerating (measuring point A1) during the first 6 milliseconds after impact with the IAEA-target the content (measuring point A2) is still moving in free fall (see also Diagram C, Figure 1). Then the internal impact between cask and fuel assembly is indicated by a relatively high deceleration of the assembly while at the same time the cask is accelerated. Diagram C shows the corresponding velocity-time histories.

The main reason for the delay or velocity difference as precondition for the internal impact appeared in the moment of release was reverse elastic spring effects of cask body and fuel assembly due to deformation energy stored in the cask components before release as discussed in [1, 2].

## **EXPERIMENTAL RESULTS – 9 m VERTICAL DROP TEST WITH A HEAVY TRANSPORT CASK FOR SPENT FUEL ELEMENTS**

As part of a BAM research project and design approval testing, a full-scale prototype of a package for transport and storage of spent fuel elements and its reduced-scale model were tested in 1 m puncture and 9 m drop tests at various cask orientations [7, 8].

The experimental results of the 9 m vertical drop test onto the lid-side of the full-scale cask are the basis of following analysis. The results are initially specified and related to the package design investigated in connection with the main drop test conditions.

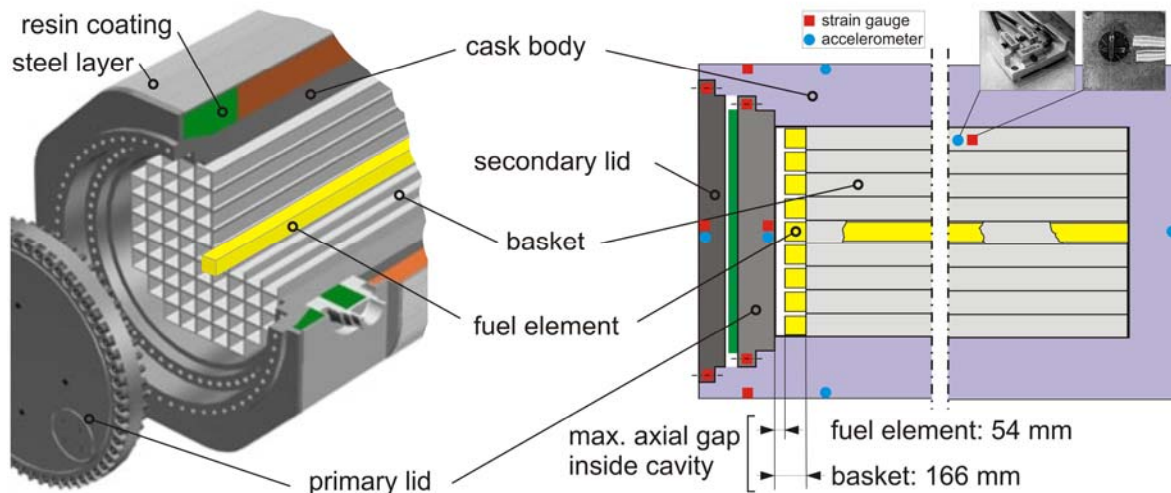
#### *Cask design/ content*

Briefly described, the package is made of a forged steel cask body closed by a bolted double lid system with metallic seals. For neutron shielding the cask body is bonded by a resin coating which is protected on the outside with a steel layer. The impact protection of the package is provided by shock absorbers in a wood composite /steel construction at the bottom- and lid-side of the cask. The package has a total mass of 127 000 kg and a total length including shock absorbers of approximately 7000 mm - Figure 2 shows a schematic view of the design.

In all drop tests the cask cavity was loaded with the corresponding basket and appropriate dummy fuel elements, simulating real fuel elements concerning outer geometry and mass (see Figure 2). The basket was built of single hollow aluminium profiles with square cross-section - the total mass of the basket amounted to 4580 kg. Every single dummy fuel element was built of a hollow steel profile representing a real fuel element's outer dimensions in length (4467 mm) and outer square cross-section (137 mm) filled with additional steel pieces fixed by welding to represent the original

mass. The single mass of an element was 305 kg – the total mass of all 69 elements 21 045 kg. Figure 2 shows the axial geometrical gaps between fuel elements, basket and primary lid of the specimen: The basket had a maximum axial gap inside the cask cavity of 166 mm – the fuel elements of 54 mm. The aluminium profiles of the basket are mounted form-fitted into the cavity so that no radial gaps occurred. The fuel elements had a small radial gap of 12 mm inside the profiles.

**Figure 2. Schematic view of the package (shock absorbers not shown), gap situation inside the cavity and instrumentation of the specimen.**



#### *Instrumentation/ drop test*

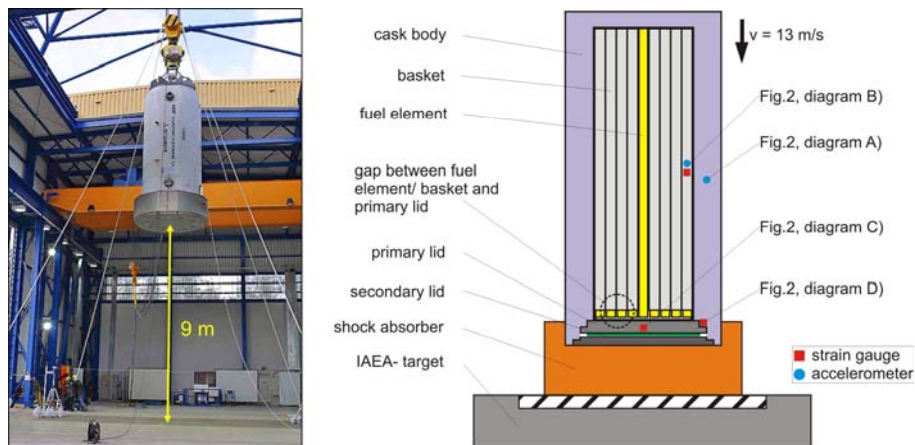
The specimen was fitted with strain gauges and accelerometers to measure with continuous monitoring the transient response of the cask and its components, respectively, due to the impact (see Figure 2). The strain gauges were located on primary and secondary lid, on the cask body, there especially in the flange region, and the basket. Four lid bolts of each lid were instrumented with strain gauges to measure pre-strain after tightening, the load during impact as well as the remaining (pre-) strain after impact. Accelerometers were mounted at the middle of the lids, at the body shell and the basket. In order to get information about the behaviour of the basket one basket-profile located in the 180°-position of the cask could be instrumented with three piezoresistive accelerometers each for one direction in space, combined with a two-axis strain gauge at the same measuring point on the half length of the profile. Due to technical reasons the dummy fuel elements could not be instrumented.

The 9 m-vertical drop test onto the unyielding IAEA-target was performed plane onto the lid-sided shock absorber so that the lid system of the cask was facing downwards. This drop orientation was chosen amongst others in order to investigate the mechanical effects of a possible internal impact of basket and fuel elements onto the lid system. Figure 3 shows on the left side the cask attached to the release system in the defined drop height of 9 meters ready for drop test and on the right side the cask directly before impact with the hypothetical situation between dummy fuel elements/ basket and primary lid.

#### *Experimental results*

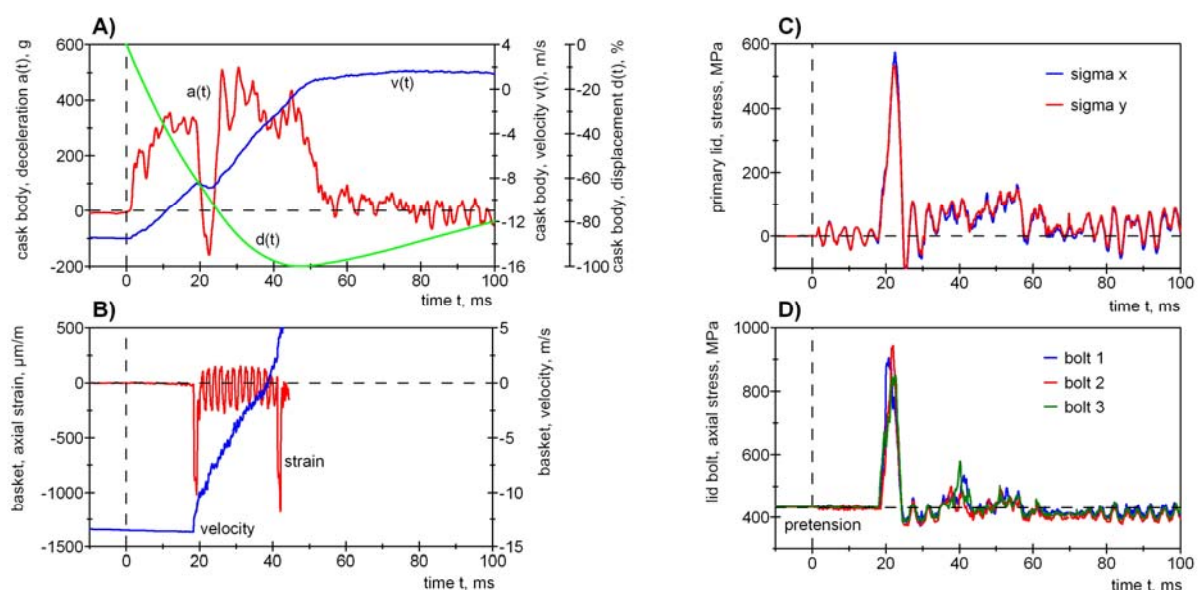
The experimental results clearly showed that an internal impact of basket and fuel elements occurred during the cask's main impact onto the IAEA-target and caused high loadings to the primary lid and its bolts. Impact responses concerning the rigid body motion of specimens are described basically by their low- pass filtered deceleration and velocity time histories. Diagram A in Figure 4 illustrates the rigid body motion vs. time of the cask in the 9 m vertical drop test during the main impact – the impact duration amounts to approximately 75 milliseconds. The significant change in cask deceleration, causing an appropriate step in the velocity time history with a temporary velocity increase of the cask is notably obvious.

**Figure 3. Drop test setup and schematic view of the casks impact situation with measuring points.**



This deceleration change, occurring in the time window between approximately 18 Milliseconds and 25 Milliseconds after the first contact of the cask with the target (time  $t = 0$ ) indicates the delayed internal impact of the dummy fuel elements and basket on the inner side of the primary lid. It can be assumed that basket and fuel elements moved relatively to the cask during the free fall using the axial clearance in the cavity and struck hardy with a delay of 18 Milliseconds onto the primary lid. This is also supported by the deceleration and strain measurements at the basket profile – Diagram B of Figure 4 shows the axial strain-time history of a basket-profile in comparison with its velocity-time history. During the first 18 milliseconds after impact of the cask the basket’s deceleration signal shows constant acceleration due to gravity ( $9.81 \text{ m/s}^2$ ) which underlines that until that time the basket moves – it is assumed that the fuel elements behave in an analogous manner – in free fall relatively to the cask as indicated in the corresponding velocity-time history (see Figure 4, Diagram B). At time  $t = 18 \text{ ms}$  the profile decelerates with a high peak value – the velocity changes – and the strain gage shows compression strain with a maximum value of  $-1000 \text{ } \mu\text{m/m}$  in longitudinal direction showing also a second impact at time  $t = 42 \text{ ms}$ . This second impact could be a kind of single event, because there is no significant and appropriate occurrence in the deceleration-time curve of the cask.

**Figure 4. Selected deceleration and strain measurement results of the 9 m-vertical drop test.**



The content impacts onto the inner side of the primary lid at a time when already 60 % of the final deformation of the shock absorber proceeded (see Figure 4, Diagram A). This internal impact

effects a high temporary loading of the primary lid and its bolts especially bending of the lid as well as bending/ tension of the lid bolts as appropriate strain measurements indicate. As an example Figure 4, Diagram C shows the stress-time history calculated from the strain signals obtained from a 2-axis strain gage rosette applicated in the middle of the primary lid. During the time period of the internal impact a significant stress peak of 550 MPa occurred - after that single event and still during the main impact of the cask the maximum values achieve not more than 150 MPa. Strain gages on the inner side of the primary lid and opposite on the top side indicate the bending of the lid.

The nominal stress of the instrumented lid bolt follows the curve progression of the stress-time history of the primary lid. Here too, the maximum stress occurred during the internal impact with a maximum peak of approximately 900 MPa (see Figure 4, Diagram D). After that no other significant loading of the bolts occurred during the remaining time of the main impact – the stresses lay in the range of the original pretension of the bolts.

The real (initial) gap between content and primary lid when the cask first hits the target is difficult to determine in the experiment. The displacements calculated by integrating twice over the accelerations acting on cask and content are inaccurate because of the accumulation of measurement uncertainties. Additionally only a basket profile could be instrumented, so that the behaviour of the dummy fuel elements must be assumed to be analogues. Nevertheless an initial gap of 35 mm was determined, which then was confirmed by the results of the analytical calculations.

## **ANALYTICAL STUDY OF THE 9 m VERTICAL DROP TEST WITH A HEAVY TRANSPORT CASK FOR SPENT FUEL ELEMENTS**

In order to gain a better understanding of the effects observed in the 9 m-vertical drop test with the full-scale cask an analytical multi-degree-of-freedom (MDOF) model was developed. The model is built of lumped masses and springs, which describe the inertia and deformation properties of the main components of the cask involved in the drop event. Figure 5 illustrates the MDOF-system schematically.

### *Shock absorber/ cask body*

Owing to the significantly lower mass and rigidity than the cask body the impacting shock absorber (lid sided shock absorber) is simulated as massless spring, whereas the cask body is considered as a single mass. The nonlinear characteristic of the spring that describes the shock absorber was derived on the basis of compression tests with wood samples [9]. The summary force-deformation-curve  $F_{sa}(x_c)$  takes the complex composite structure of the shock absorber (three kinds of wood with different grain orientation) into account. The mass  $m_c$  connected with this spring is the sum of the mass of the cask body, secondary lid and the bottom sided shock absorber.

### *Dummy fuel assemblies/ basket*

The basket is built of  $n_b = 69$  separate hollow aluminium profiles in which  $n_d = 69$  steel dummy fuel elements are placed. Additional steel pieces are welded to the dummies to fit their weights to the ones of real fuel elements. For both, basket profiles and fuel elements the longitudinal dimension is far larger than their cross-sectional dimensions and the stiffness distribution from top to end is nearly homogeneous. The elastic response of such bar-like structures to a longitudinal impact can be represented by MDOF systems with a finite number of concentrated masses connected in series by means of linear springs. Previous calculations showed that the contact force-time history of a homogeneous bar striking an unyielding target is sufficiently described by a 4-DOF mass spring system, at least for the problem in hand. But this discretisation level could only be used for the basket. The dummy fuel elements, due to additional weights added and some irregularity in the stiffness distribution, are simulated by 6-DOF systems.

The internal impact is assumed to be synchronous for all basket profiles and all dummy fuel elements. That means, basket as well as dummy fuel elements are considered as one summarised 4-DOF system and one summarised 6-DOF system, respectively. In order to obtain the combined characteristics of these MDOF- systems the corresponding spring constants and masses of the basket ( $k_{bi}, m_{bi}$ ) and dummy fuel elements ( $k_{di}, m_{di}$ ) are summarised as follows:

$$\begin{aligned} \text{basket:} \quad & k_{bi} = n_b \frac{E_b \cdot A_{bi}}{L_{bi}}; \quad m_{bi} = n_b (\rho_b \cdot A_{bi} \cdot L_{bi} + \Delta m_{bi}); \quad m_b = \sum_1^4 m_{bi}; \quad i = 1, 2, \dots, 4 \\ \text{fuel elements:} \quad & k_{di} = n_d \frac{E_d \cdot A_{di}}{L_{di}}; \quad m_{di} = n_d (\rho_d \cdot A_{di} \cdot L_{di} + \Delta m_{di} + m_{add}); \quad m_d = \sum_1^6 m_{di}; \quad i = 1, 2, \dots, 6 \end{aligned}$$

where  $E_b, (E_d)$  and  $\rho_b, (\rho_d)$  are the Young's modulus of elasticity and the density of the basket's (fuel element's) material,  $A_{bi}, (A_{di})$  and  $L_{bi}, (L_{di})$  are the section area and length of the  $i$ -th segment of a basket tube (fuel element) and  $\Delta m_{bi}, (\Delta m_{di})$  are the correction terms to adapt the mass of the MDOF system to the real mass of the structure. The additional term  $m_{add}$  considers the mass fixed within the  $i$ -th segment of the dummy fuel element.

The force characteristics of the base springs of basket  $F_{b1}(x)$  and dummy fuel elements  $F_{d1}(x)$ , which interact directly with the primary lid during the internal collision, have to take into account the possible separation of their contact with the lid and are defined by distinction of cases as follows

$$F_{b1}(x) = \begin{cases} 0, & x \leq 0 \\ k_{b1}x, & x > 0 \end{cases} \quad \text{and} \quad F_{d1}(x) = \begin{cases} 0, & x \leq 0 \\ k_{d1}x, & x > 0 \end{cases}$$

#### Primary lid system

The primary lid is mounted to the flange of the cask body with in total  $n_s = 48$  bolts having the preload (pretention)  $F_V$  in the defined assembly state.

The mass of the lid bolts is small in comparison with the mass of the lid and so the bolted joints can be described as  $n_s$  massless springs connected in parallel. In this approximation only the tension/compression resistance of the bolted joints (i.e. combined characteristic of preloaded lid bolts with corresponding clamped parts of the flange) is taken into account. The bending resistance is assumed to be negligible and is ignored here. If the assembly state is chosen as initial point for spring deformation, the summary nonlinear force characteristic of the joints will be given by the equation

$$F_j(x, F_V) = n_s \begin{cases} -F_V + \frac{x}{\delta_p}, & x \leq -\Delta_s \\ \frac{x}{\delta_s \Phi}, & -\Delta_s \leq x \leq |\Delta_p| \\ F_V + \frac{x}{\delta_s}, & x \geq |\Delta_p| \end{cases}$$

where  $\delta_s$  and  $\delta_p$  are the elastic resiliencies of the bolt and the clamped part, and  $\Phi = \delta_p / (\delta_s + \delta_p)$  is the load factor of the joint assumed as concentric clamped and loaded [10]. The values  $\Delta_s = \delta_s F_V$  and  $\Delta_p = -\delta_p F_V$  are the initial tension of the bolt and initial compression of the clamped part in assembly state. The force characteristic of the joint should be distinguished from the bolt force defined by equation

$$F_s(x, F_V) = \begin{cases} 0, & x \leq -\Delta_s \\ F_V + \frac{x}{\delta_s}, & x \geq -\Delta_s \end{cases}$$

The primary lid is assumed as simply-supported elastic circular plate with constant thickness  $t_l$ . It can be supposed that the first mode predominates in dynamic response of the lid in

vertical drop orientation. Reasonably accurate results can be obtained by considering only this mode. Alternatively, a deflected shape caused by a uniform distributed load applied statically (dead-weight load) can be used for this purpose.

By means of the procedure described in [11] the equivalent mass  $m_l$  and the spring constant  $k_l$ , of the single-degree-of-freedom (SDOF) system approximated the dynamic response of the plate can be calculated as:

$$m_{el} = \pi R^2 \gamma \frac{5(7+\nu)^2}{3(113+36\nu+3\nu^2)}, \quad k_{el} = \pi \frac{D}{R^2} \frac{1600(1+\nu)(7+\nu)^3}{3(113+36\nu+3\nu^2)^2}$$

with mass per unit area  $\gamma$ , flexural rigidity  $D = \frac{E_l \cdot t_l^3}{12(1-\nu^2)}$ , Young's modulus of elasticity  $E_l$  and Poisson's ratio  $\nu$  of the lid material. The consideration of the spring  $k_{el}$  as connected in series with the spring of the bolted joint  $F_j(x, F_V)$  leads to the combined spring characteristic of the lid system  $F_{ls}(x, F_V)$ .

#### Dynamic model of the cask

The system of equations of motion for the whole structure has the following form:

$$\begin{aligned} (m_c + m_{lr})\ddot{x}_c + F_{sa}(x_c) - F_{ls}(\bar{x}_l, F_V) &= 0 \\ m_{el}\ddot{\bar{x}}_l + F_{ls}(\bar{x}_l, F_V) - F_{b1}(\Delta_{b1}) - F_{d1}(\Delta_{d1}) \\ &= -\alpha\ddot{x}_c m_{b1}\ddot{\bar{x}}_{b1} + F_{b1}(\Delta_{b1}) - k_{b2} \cdot (x_{b2} - x_{b1}) = 0 \\ m_{b2}\ddot{x}_{b2} + k_{b2} \cdot (x_{b2} - x_{b1}) - k_{b3} \cdot (x_{b3} - x_{b2}) &= 0 \\ m_{b3}\ddot{x}_{b3} + k_{b3} \cdot (x_{b3} - x_{b2}) - k_{b4}x_{b4} &= 0 \\ m_{b4}\ddot{x}_{b4} + k_{b4}x_{b4} &= 0 \\ m_{d1}\ddot{x}_{d1} + F_{d1}(\Delta_{d1}) - k_{d2} \cdot (x_{d2} - x_{d1}) &= 0 \\ m_{d2}\ddot{x}_{d2} + k_{d2} \cdot (x_{d2} - x_{d1}) - k_{d3} \cdot (x_{d3} - x_{d2}) &= 0 \\ \dots \\ m_{d5}\ddot{x}_{d5} + k_{d5} \cdot (x_{d5} - x_{b4}) - k_{d6}x_{d6} &= 0 \\ m_{d6}\ddot{x}_{d6} + k_{d6}x_{d6} &= 0 \end{aligned}$$

with

$$x_l = x_c + \bar{x}_l, \quad \Delta_{b1} = \beta \cdot (x_{b1} - x_l) \quad \text{and} \quad \Delta_{d1} = \beta \cdot (x_{d1} - x_l).$$

The factors  $\alpha$  and  $\beta$  are defined in [11] as

$$\alpha = m_{el} \quad \text{and} \quad \beta = \frac{5(7+\nu)^2}{3(113+36\nu+3\nu^2)}.$$

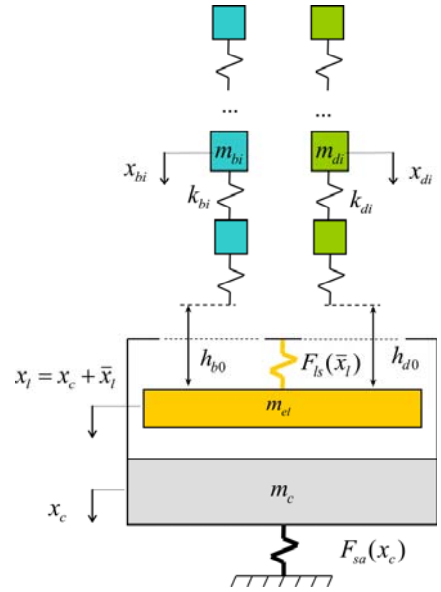


Figure 5. MDOF- model of the cask.



These factors are needed for the proper connection of the equivalent oscillator, which replaced the lid system, in the whole dynamic model of the cask. The initial conditions for the equations of motion are

$$t = 0, \quad x_c = 0, \quad \dot{x}_c = v_0; \quad \bar{x}_l = \dot{\bar{x}}_l = 0;$$

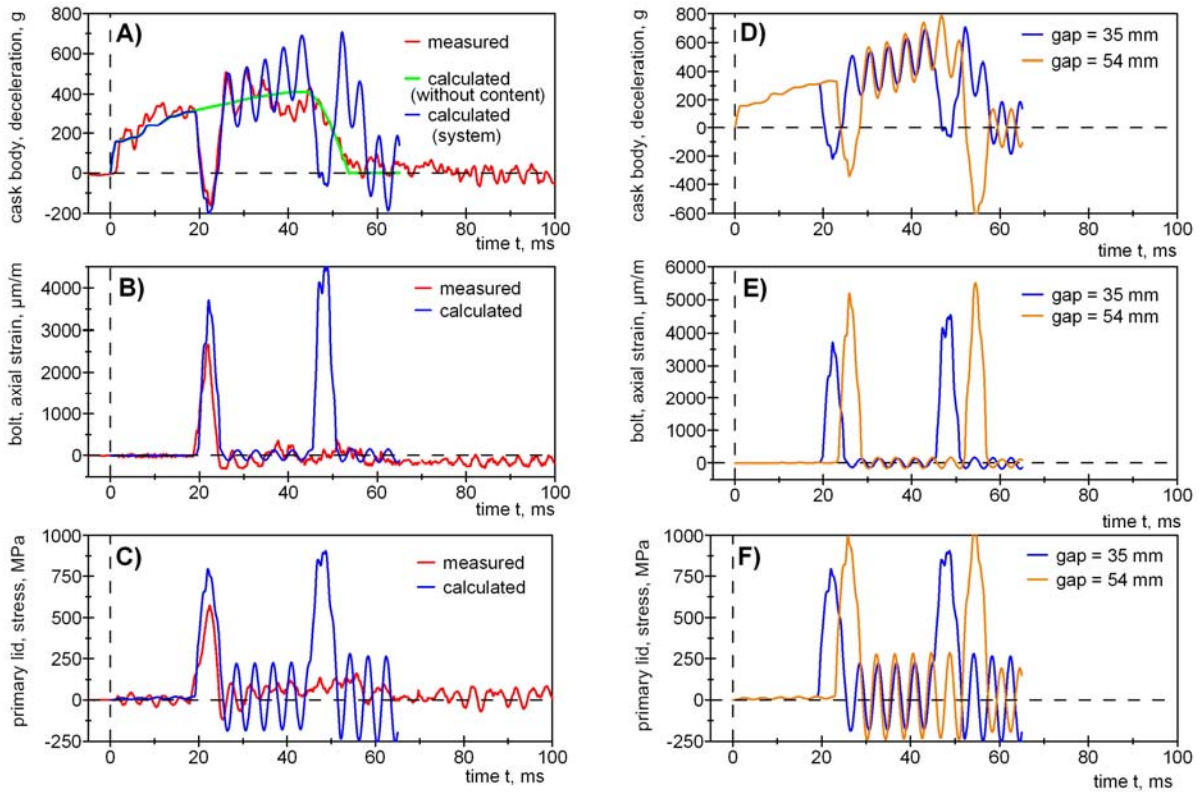
$$x_{bi} = h_{b0}, \quad \dot{x}_{bi} = v_0, (i = 1, 2, \dots, 4); \quad x_{di} = h_{d0}, \quad \dot{x}_{di} = v_0, (i = 1, 2, \dots, 6)$$

where  $v_0$  is the initial velocity resulting from the vertical free fall of the cask,  $h_{b0}$  and  $h_{d0}$  are the initial distances from the basket and the dummy content to the inner side of the primary lid.

#### Results/ comparison with the experimental data of the 9m vertical drop test

The numerical solution of the equations of motion - performed with “Mathematica” [12] - was started with a variation of the initial distances  $h_{b0}$ ,  $h_{d0}$  between content and primary lid in order to achieve the content’s delayed impact of 18 milliseconds as in the experiment. The result of the parameter variation was a gap of 35 mm. This value corresponds perfectly with the initial gap between content and primary lid determined in the experiment for first hits of the cask onto the target.

**Figure 6. Diagrams A, B, C compare results between experiment and calculation – Diagrams D, E, F calculation data between determined gap (35 mm) and maximum possible gap (54 mm).**



In the following step the calculations were carried out with an initial gap of 35 mm as initial condition:  $h_{b0} = h_{d0} = 35 \text{ mm}$ . The pretension of the lid bolts was assumed to be equal to the average tensile stress value measured at the instrumented bolts during the assembly of the primary lid before the vertical drop test. Apart from this the geometrical dimensions and masses of the specimen were used. Diagram A in Figure 6 shows the calculated deceleration time history of the cask body in comparison with the experimental results - the green curve represents additionally the deceleration of the cask assumed as empty. Diagrams B and C show the bending stress in the middle of the primary lid and the additional strain (relative to the assembly state) in the primary lid bolts, respectively.

The calculation results are in good agreement with the experiment and correlate well with the measured decelerations and strains before and during the internal impact phase. Due to the fact that damping effects are not considered in the MDOF-model the numerical and experimental results deviate after the internal impact increasing with time, so that the MDOF-model shows another internal impact approximately 25 milliseconds after the ‘first impact’.

It is obvious that after the first internal impact in the drop test, the basket profiles and the dummy fuel elements moved separately from each other and therefore the effects of following collisions of these parts with the primary lid were smoothed. By contrast in the numerical simulation both the basket and the dummy content are assumed to move as units after the first internal impact as well, and so the second internal impact at time  $t \sim 46$  ms can be clearly seen. The higher loadings of the primary lid and lid bolts obtained in the calculations can be attributable to the fact that the secondary lid is not included in the model and its supporting action on the primary lid observed in the drop test is not simulated as well.

Despite these deviations it may be deduced that the MDOF-model describes the main physical effects during the vertical drop test correctly and sufficiently accurate. The model can therefore be used as an additional calculation tool for the comparison study of different parameter combinations essential for the tested cask (initial gaps, bolt pretension, etc.).

In the last calculation step the initial gap was set to the maximum value which is possible for the fuel elements, i.e.  $h_{b0} = h_{d0} = 54$  mm. The results show an increase of the primary lid and bolts loadings by approximately 30 % and 45 % relating to the drop test results. Diagram D of Figure 6 show the calculated cask decelerations vs. time in comparison between real gap as in the drop test (35 mm) and the maximum possible gap (54 mm) – Diagram E and F show the calculated stresses in the middle of the primary lid and the axial strain of the primary lid bolts also relating to the gaps of 35 mm and 54 mm.

## CONCLUSION

In transport casks for radioactive materials technological gaps between basket or radioactive content and cask body or primary lid can be a reason for significant high dynamic loadings of cask components and its internals due to additional impact interactions in the cask cavity. The deformation energy stored in the cask structure before release and the momentum which results from loss of deformation after release was identified as the main cause for different motion of the cask and its content during the free fall phase with subsequent internal impact interactions during the main impact onto the target. The parameters governing these interactions are of a rather random nature, so that the internal impact is more or less noticeable in real tests. Any adjustment of the cask and its content relative to one another in the “before drop” configuration - e.g. setting the maximum possible gaps - is not practicable, especially in drop tests with full scale models of heavy casks. On the other hand, just due to a multitude of the governing parameters an only numerical analysis of this subject seems to be uncertain. In this context the combination of drop tests with post-test numerical analysis is generally preferred in order to estimate the effects of internal impacts in a realistic way.

## REFERENCES

- [1] Quercetti, T. *et al.* (2003). *Interactions between cask components and content of packaging for the transport of radioactive material during drop tests*. 17th International Conference on Structural Mechanics in Reactor Technology (SmiRT 17), August 17-22, 2003, Prague, Czech Republic (Proceedings) – Paper # J07-1 (2003), 8 pages
- [2] Ballheimer, V. *et al.* (2002). *Effects and consequences of interactions between containment components and content of type B packages during 9 m drop tests*. ‘RAMTRANS’ Vol.130, No. 3-4, pp. 305-312, Nuclear Technology Publishing.
- [3] Quercetti, T. *et al.* (2007). Comparison of experimental results from drop testing of spent fuel package design using full scale prototype model and reduced scale model.

- [4] Purcell, P. (2010). *Analysis of impact induced accelerations on internal components of light water reactor packages*. Packaging, Transport, Storage and Security of Radioactive Material, 21, (3), 142-146.
- [5] Bjorkman G. (2009). *The effect of gaps on the impact response of a cask closure lid*. ASME PVP 2009-77800 (Pressure Vessels and Piping Conference), Prague.
- [6] Hilbert, F. *The ESBB Package for the Transport and Interim Storage of MOX Fuel Assemblies and Pins*. The 13th International Conference on Packaging and Transportation of Radioactive Materials, September 3-8, 2001; Chicago, Illinois, USA; Revised Proceedings, paper 33393 (CD)
- [7] Tamaki, H. *et al.* (2006). *Results of Full-scale drop tests for "MSF spent nuclear fuel transport and storage cask in Germany*. INMM Spent Fuel Management Seminar XXIII, January 11-13, Washington D.C., USA
- [8] Droste, B. *et al* (2009). *Fallversuche mit Brennelement-/HAW-Transport- und Lagerbehältern in Originalgröße*. Abschlußbericht zum Forschungsvorhaben mit dem BMBF-Förderkennzeichen 02S8274 (BAM-Vorhaben Nr.3311), Berlin, September 2009
- [9] Kishimoto J. *et al.* (2007). *Dependency of Temperature on Wooden Materials' Mechanical Property and Effect of Impact Energy Absorption of Shock Absorbers*. Proc. 15<sup>th</sup> Int. Symp. on 'Packaging and Transportation of Radioactive Materials (PATRAM 2007)', Paper 267, Miami, Florida, USA , October 2007.
- [10] Verein Deutscher Ingenieure (VDI): *Systematic calculation of high duty bolted joints: joints with one cylindrical bolt, VDI 2230*. VDI-Gesellschaft Entwicklung Konstruktion Vertrieb, Düsseldorf, Germany, February 2003.
- [11] Ballheimer, V. (2012). *Simplified modelling of a cask lid in internal collision problem*. BAM, Berlin, April 2012 (unpublished note)
- [12] Wolfram, S. (2003) *The Mathematica Book*, Wolfram Media, Inc, 5th Edition